Magnetic conjugacy of northern and southern auroral beads

Tetsuo Motoba,[1] Keisuke Hosokawa,[2] Akira Kadokura,[1] and Natsuo Sato[1]

Received 5 March 2012; accepted 26 March 2012; published 25 April 2012.

[1] Auroral beads, i.e., azimuthally arrayed bright spots resembling a pearl necklace, have recently drawn attention as a possible precursor of auroral substorms. We used simultaneous, ground-based, all-sky camera observations from a geomagnetically conjugate Iceland-Syowa Station pair to demonstrate that the auroral beads, whose wavelength is ∼30–50 km, evolve synchronously in the northern and southern hemispheres and have remarkable interhemispheric similarities. In both hemispheres: 1) they appeared almost at the same time; 2) their longitudinal wave number was similar ∼300–400, corresponding bead separation being ∼1° in longitude; 3) they started developing into a larger scale spiral form at the same time; 4) their propagation speeds and their temporal evolution were almost identical. These interhemispheric similarities provide strong evidence that there is a common driver in the magnetotail equatorial region that controls the major temporal evolution of the auroral beads; thus, the magnetosphere plays a primary role in structuring the initial brightening arc in this scale size. **Citation:** Motoba, T., K. Hosokawa, A. Kadokura, and N. Sato (2012), Magnetic conjugacy of northern and southern auroral beads, *Geophys. Res. Lett.*, *39*, L08108, doi:10.1029/2012GL051599.

1. Introduction

[2] Since a global morphology of auroral substorms was first introduced by *Akasofu* [1964], our understanding of them has progressed significantly. However, the nature of the mechanism that initiates the explosive onset of auroral breakup is still controversial. Recently, attention has been drawn to the temporal evolution of the initial brightening arc during the few minutes before the onset, because it could illustrate the process that triggers the expansion phase onset. Optical observations from the ground [*Donovan et al.*, 2006; *Liang et al.*, 2008; *Sakaguchi et al.*, 2009] and from spacecraft [*Elphinstone et al.*, 1995; *Henderson*, 2009] have shown that in the initial brightening arc, there exists a characteristic small-scale auroral structure, consisting of azimuthally arrayed wave-like forms (often referred to as "auroral beads") with a wavelength of 30–100 km and an azimuthal propagation speed of 5–8 km s^{-1}. As time progresses, the auroral beads evolve into wave-like undulations with a larger scale of 50–200 km, and finally lead to auroral breakup. In order to reveal the temporal evolution of such structures, several case studies using ground-based all-sky cameras have been performed in recent years [*Sakaguchi et al.*, 2009, and references therein]. However, it is still unknown whether they always appear prior to auroral breakup because there has been no statistical survey using a large number of case examples. Using optical observations from space, on the other hand, *Elphinstone et al.* [1995] demonstrated that similar azimuthally spaced auroral forms were identified for 26 out of 37 substorms. This implies that the bead-like auroral structures could be a common morphological feature in the pre-onset interval. Although the mechanism producing the auroral beads is still controversial, some of the previous studies suggested that the beads are a manifestation of magnetospheric instability in the plasma sheet [*Cheng*, 2004]. Thus far, however, there have been no observations to support this idea. In particular, we have not been able to eliminate the possibility that the auroral beads are produced by a process working somewhere between the magnetosphere and ionosphere (within or below the auroral acceleration region).

[3] In this report, we present a case in which the auroral bead structures were observed simultaneously by two white light all-sky cameras (ASCs) at a pair of geomagnetically conjugate sites: Tjörnes in Iceland (66.20°N, 342.89°E, geomagnetic latitude [GMLat]: 66.27°N) and Syowa Station (69.00°S, 39.58°E, GMLat: 66.33°S) in Antarctica (cf. *Motoba et al.* [2010] for more details of the instruments and sites). If the northern and southern aurorae are nearly symmetric (i.e., magnetically conjugate), their spatial and temporal features simply reflect the evolution of the common source in the magnetosphere (any disturbance/instability). However, if they are asymmetric, there must be some additional structuring processes at lower altitudes that can induce non-conjugate auroral behavior. In either case, auroral observations at conjugate points can provide important clues to understanding the characterization of various types of aurora. In particular, conjugate observations of the initial brightening arc can help us to distinguish the source of the auroral beads.

2. Observations

[4] On the night of September 30, 2011, we succeeded in recording a remarkable case of conjugate auroral breakup. Let us first look at the prevailing interplanetary and geophysical conditions for the 30 September 2011 substorm event. Figures 1a and 1b respectively show the interplanetary magnetic field (IMF) variations time-shifted to the dayside magnetopause and the provisional AU/AL indices between 22:00 and 24:00 UT on September 30, 2011. The IMF data measured by the fluxgate magnetometer onboard THEMIS B [*Auster et al.*, 2008] in the upstream solar wind at (39.0, 40.9, −11.6) R_E in GSM coordinates were time-shifted with a lag of 13 min to account for the time delay from THEMIS B to THEMIS D near the dayside

[1]National Institute of Polar Research, Tachikawa, Japan.
[2]Department of Communication Engineering and Informatics, University of Electro-Communications, Chofu, Japan.

Corresponding Author: T. Motoba, National Institute of Polar Research, 10-3 Midori-cho, Tachikawa, Tokyo 190-8518, Japan. (motoba.tetsuo@nipr.ac.jp)

0094-8276/12/2012GL051599

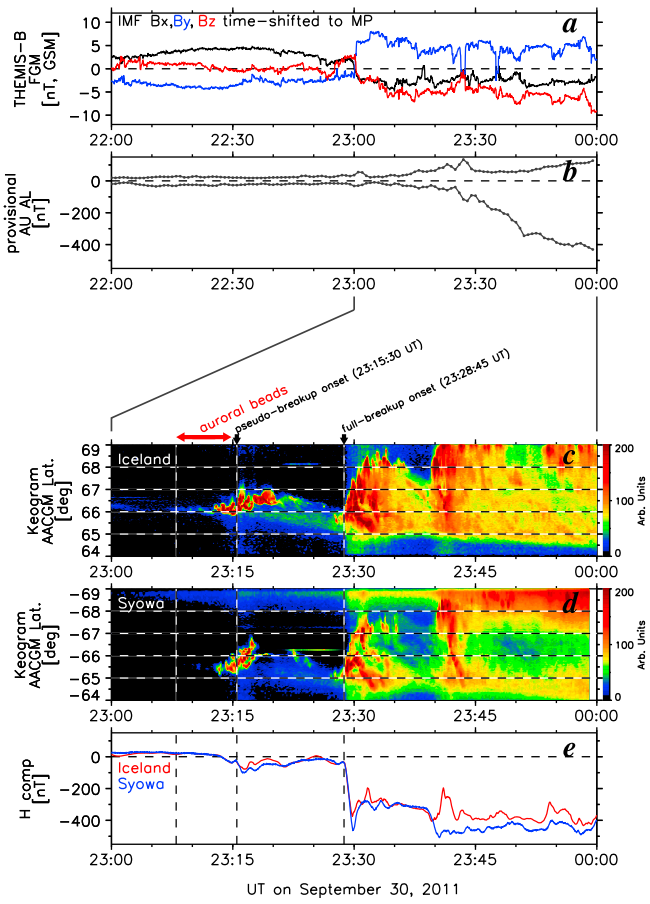

Figure 1. An overview of the 30 September 2011 substorm event: (a) IMF Bx, By, and Bz time-shifted to the dayside magnetopause (see text for details), (b) provisional AU and AL indices, (c) S-N keogram from Iceland, (d) N-S keogram from Syowa, and (e) ground H component magnetograms in Iceland and Syowa.

magnetopause at (6.5, 9.4, 2.1) R_E. At around 23:00 UT, a southward turning of IMF reached the dayside magnetopause, and after that the southward IMF condition remained for about 30 min. During this period of southward IMF, AU/AL indices showed a typical signature of substorm growth phase. Around 23:30 UT, at which a small excursion of IMF Bz from negative to ~0 was observed, an expansion phase onset occurred, which is marked by a start of significant AL index decrease. Figures 1c–1e respectively show keograms reproduced from the all-sky images in Iceland and Syowa along the south-north cross-section, and 1 s H component ground magnetograms at both stations between 23:00 and 24:00 UT. In Figures 1c and 1d, there can be identified two poleward expansions: small/localized one at 23:15:30 UT (probably classified as a pseudo breakup) and subsequent full expansion at 23:28:45 UT. These poleward expansions were accompanied by negative deflections in the ground magnetic field of about −50 nT and −400 nT, respectively. It is clearly seen that the optical and magnetic field signatures of substorm were very similar in both stations throughout the interval. In this study, we focus on the 7-min period before the localized poleward expansion at 23:15:30 UT, during which the auroral bead structures appeared simultaneously in both hemispheres.

[5] Figure 2a shows an example of the conjugate auroral beads observed simultaneously in Iceland (left) and Syowa (right) at 23:09:40 UT. Five outstanding auroral beads are labeled with letters *a–e.* The positions of the labels were mapped along the geomagnetic field lines given by the Tsyganenko 96 (T96) magnetic field model [*Tsyganenko and Stern*, 1996] that potentially includes the IGRF model. We used IMF By = 4.6 nT, Bz = 0 nT, Dst = 0 nT, and Pdyn = 2 nPa as input parameters for the field line tracing. We will discuss the choice of these input values and difficulties in the mapping process later in this section. The temporal evolution of the beads can be seen more clearly in Animation S1 in the auxiliary material.[1] The animation shows that the auroral beads appeared almost simultaneously in both hemispheres and moved eastward synchronously until the start of the localized poleward expansion at 23:15:30 UT.

[6] The magnetic conjugacy of the northern and southern auroral beads was investigated in further detail via a comparison of these beads in a narrow conjugate area within the field of view (FOV) indicated by the dotted red border. Figure 2b shows the Iceland image (left) in the narrow area in the northern hemisphere (66.25° ± 0.5° GMLat and 72.0° ± 4.5° GMLon), and the Syowa image (right), which has been mapped onto the northern area using the T96 model with the input parameters described above. Both images are projected onto an assumed auroral emission altitude of 110 km and depicted as a function of GMLon and GMLat. The gray-shaded area corresponds to a region outside the 60° zenith angle of each ASC FOV. A closer look at their distributions reveals that the Icelandic auroral beads have an almost one-to-one correspondence with the Antarctic beads. The marked auroral beads were distributed longitudinally within the narrow range of latitudes from 65.9° to 66.25° GMLat (~35 km). The average scale of each bead segment in the longitudinal direction was roughly 30–50 km, while the separation between neighboring beads was roughly 50–80 km. Figure 2c shows the longitudinal profiles of the auroral bead brightness in Iceland (black) and Syowa (gray), which were derived by averaging the data from 65.9° to 66.25° GMLat in Figure 2b. Again, a remarkable one-to-one correspondence between individual bead locations is seen, especially for the beads *b–d.* However, the correspondence between the northern and southern beads is slightly unclear for the beads *a* and *e.* This is due to the averaging scheme over the beads tilted in latitude, which makes it hard to identify these beads in the longitudinal profiles of the brightness.

[7] The temporal evolution of the auroral beads in the narrow conjugate area from 23:08:00 UT to 23:15:00 UT is shown in Figure 3a (Iceland) and Figure 3b (Syowa), with a time resolution of 20 s. The upper and lower panels correspond to two intervals: from 23:08:00 UT to 23:11:20 UT, and from 23:11:40 UT to 23:15:00 UT, respectively. In order to highlight the auroral bead structures with relatively weak luminosity, different color scales are used for the former and latter intervals. When we mapped the Syowa images onto the northern hemisphere with the T96 model, we used slightly different IMF By values as an input for the model. This is because the geometry of the tail field lines

[1]Auxiliary materials are available in the HTML. doi:10.1029/2012GL051599.

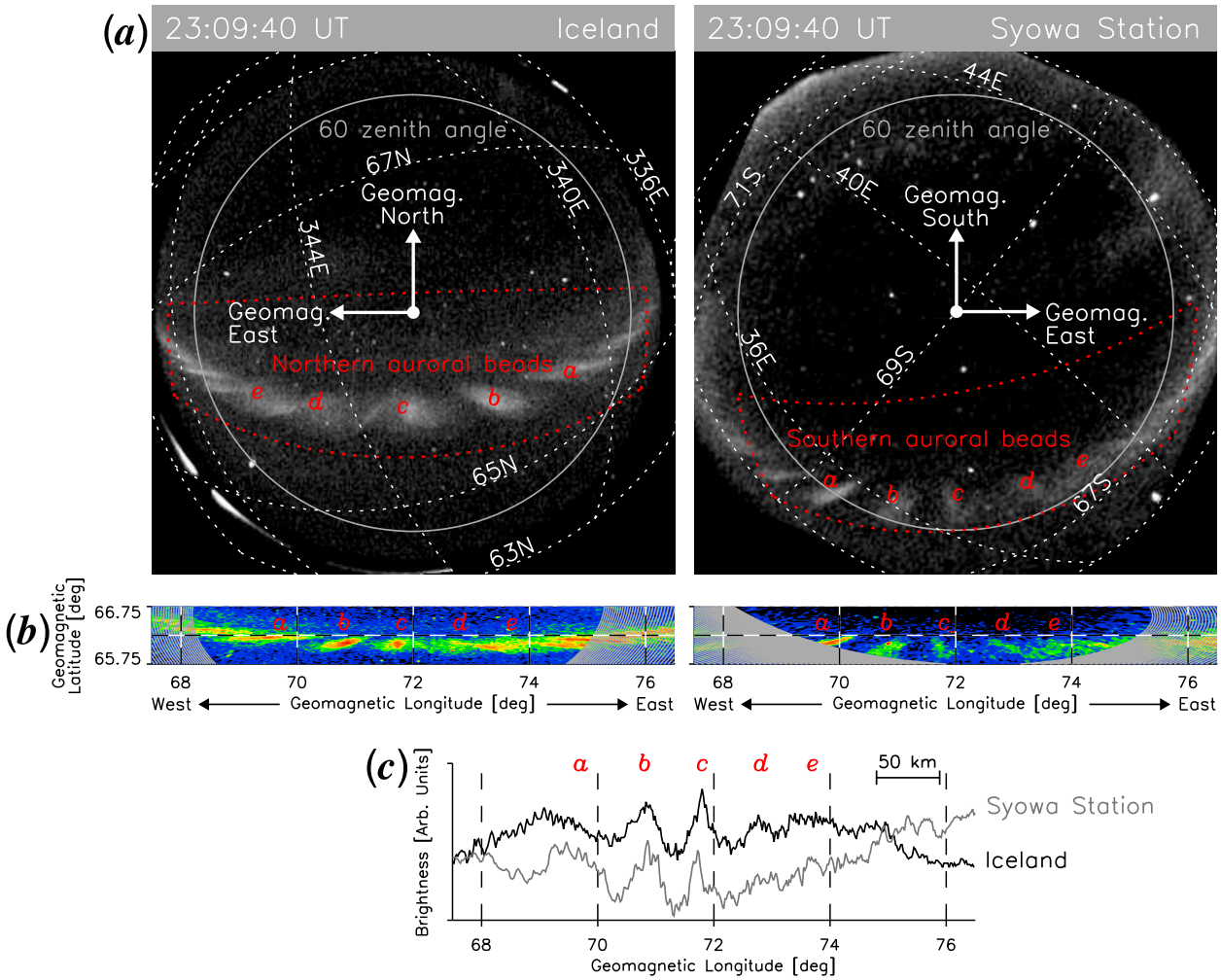

Figure 2. (a) ASC images taken simultaneously in (left) Iceland and (right) Syowa at 23:09:40 UT on September 30, 2011. The top is directed toward the magnetic pole. Dotted lines indicate geographic latitudes and longitudes, and the gray circle represents the 60° zenith angle. Five examples of the auroral beads connected along the geomagnetic field lines are labeled *a*–*e* in the ASC images. (b) A zoomed-in view of the auroral beads, color-coded with arbitrary units, in the geomagnetically conjugate area indicated by the red dotted border in Figure 1a. See text for details of the format. (c) Longitudinal profiles of the averaged auroral bead brightness in Iceland (black) and Syowa (gray). The averages are between 65.9° and 66.25° GMLat where the major auroral beads are located.

and the resulting conjugate points are known to change very dynamically [e.g., *Motoba et al.*, 2010]. This makes it rather difficult to do the mapping with fixed input parameters, even for a short interval. Thus, we chose different IMF By values ranging from 3.3 nT to 6.3 nT for each image, so that the location of the most outstanding bead *b* in the Syowa images well matches that in the Iceland images.

[8] Before the formation of the auroral beads (23:08:00 UT), a stable east-west aligned auroral arc was present along a GMLat of around 66° in both hemispheres. A few tens of seconds later, the longitudinally separated bead structures started forming almost simultaneously in the preexisting northern and southern arcs. For reference, the beads labeled in Figure 2 are marked by the corresponding letters, and for the beads *b* and *c* their trails are roughly traced by dashed white slopes. Note that these dashed lines only give an approximate guide for tracking the temporal evolution of the beads by eye and were not used for any further analyses. By averaging the longitudinal displacements of all identifiable bead peaks between consecutive images every 10 s, we estimated the average eastward propagation speeds of the northern (red) and southern (blue) auroral beads, which are shown in Figure 3c. In the first 4 min, both eastward propagation speeds were almost identical and were constant at 1 km s^{-1} or less. Figure 3d gives the temporal variations of the auroral brightness in Iceland and Syowa, which were derived by averaging the data within the fixed area of latitudes from 65.9° to 66.25° GMLat and longitudes from 70.0° to 74.0° GMLon.

[9] The conjugate auroral beads underwent a two-step evolution: during the first ~4 min, from 23:08:40 UT to 23:12:20 UT, the beads moved eastward gradually, maintaining well-organized azimuthal structures. The size and luminosity remained relatively uniform throughout this slow development stage. After the slowly developing stage, the beads became more active after 23:12:40 UT. During the active stage, the beads brightened, and their propagation speed increased. Figure 3c shows that the average

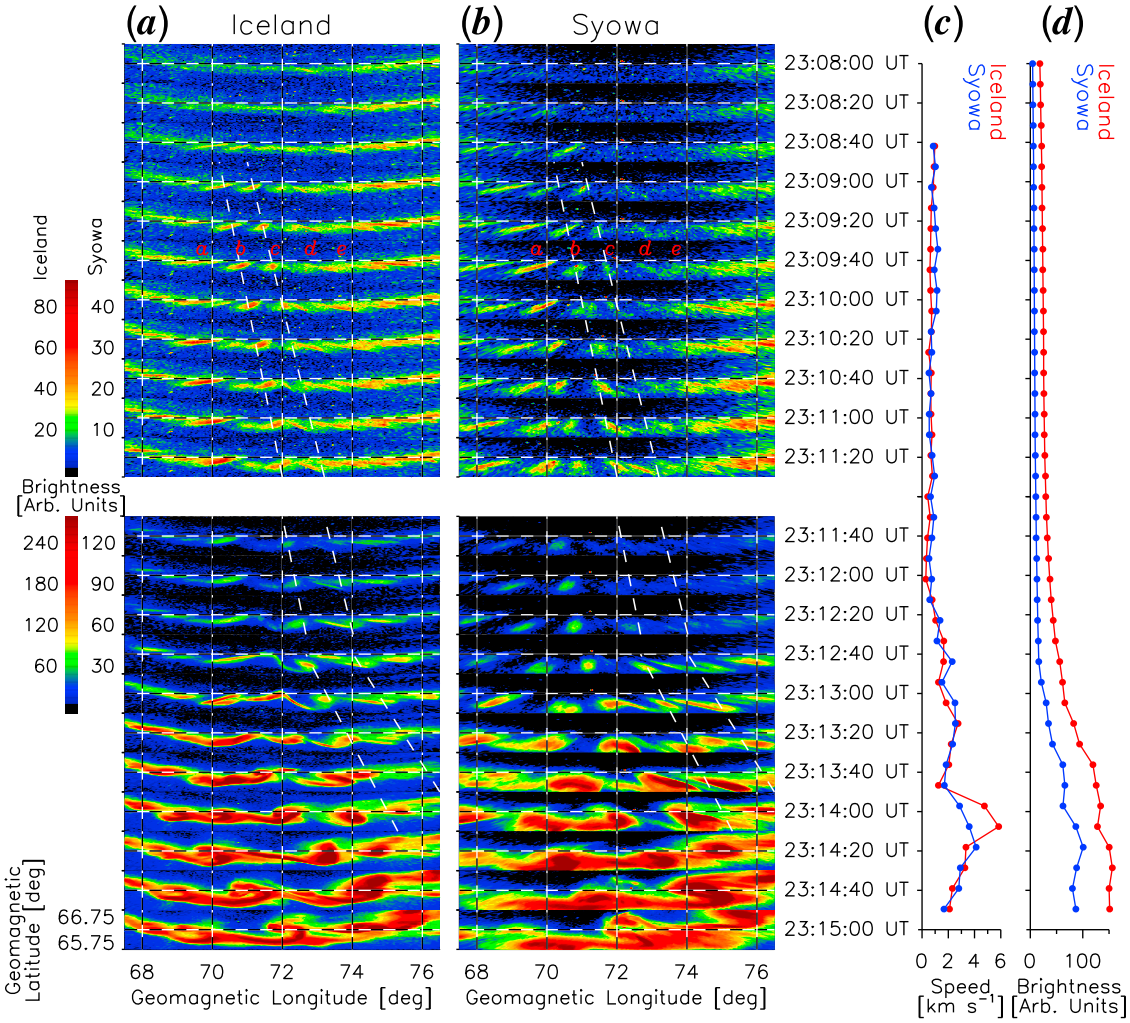

Figure 3. Time sequence of the conjugate auroral beads observed (a) in Iceland and (b) at Syowa Station every 20 s for the 7-min interval from 23:08:00 UT to 23:15:00 UT. The individual panels have the same format as Figure 2b. The labeled beads (*a*–*e*) at 23:09:40 UT correspond to those shown in Figure 2. For reference, temporal evolution of the auroral beads (*b* and *c*) is roughly traced by dotted white slopes. The aurora brightness is color-coded according to the scales on the left side. (c) Average eastward propagation speeds and (d) average brightness variations of the northern (red) and southern (blue) auroral beads.

propagation speed during the active stage was 2–6 km s^{-1}, which is comparable to that reported in previous studies [*Donovan et al.*, 2006; *Sakaguchi et al.*, 2009]. In addition, the neighboring beads merged into the spiral-like structure with a larger spatial scale. At 23:15:00 UT, the longitudinal scale of the spiral-like aurora was about 2–3 times larger than that of the initial auroral beads. Although the northern and southern aurorae changed their forms drastically during the active stage, they still showed good magnetic conjugacy. Subsequently, both aurorae developed into the localized poleward expansion within about 1 min after 23:15:00 UT.

3. Discussion and Conclusion

[10] The auroral beads during the current interval have the following characteristics: 1) they appeared at almost the same time in both hemispheres; 2) their longitudinal wave number was similar ~300–400, corresponding bead separation being ~1° in longitude, in both hemispheres; 3) they started developing into a large-scale spiral form at the same time in both hemispheres; 4) their propagation speeds and their temporal evolution were identical in both hemispheres. Moreover, it is obvious in Animation S1 that the beads' structures evolved synchronously in both hemispheres, maintaining these remarkable similarities. Due to the uncertainty in the accuracy of the field line tracing, it is impossible to conclude that the location of the beads always had an exact one-to-one correspondence between the two hemispheres. However, the abovementioned interhemispheric similarities strongly suggest that there must be a common driver in the magnetotail equatorial region that was controlling the major temporal evolution of the auroral beads. Most of the previous studies of auroral beads [e.g., *Donovan et al.*, 2006; *Liang et al.*, 2008] inferred that the magnetospheric driver of the auroral beads may be a ballooning type instability [*Cheng*, 2004]. Of course, some different processes at a lower altitude along the field line (i.e., M-I coupling region) may also contribute to the structuring of the bead structures: for example, ionospheric feedback instability in the so-called ionospheric Alfven

resonator [*Lysak and Song*, 2002] and instabilities in the auroral acceleration region [*Chaston and Seki*, 2010]. Considering the remarkable interhemispheric similarities in the characteristics of the auroral beads, however, the contribution of such processes would be relatively minor. That is, the magnetosphere plays a primary role in determining the temporal evolution of the auroral beads.

[11] By projecting the all-sky images onto the magnetotail equatorial plane using the T96 model, we attempted to deduce a first-order estimate for the bead parameters in the magnetosphere. We found that the beads were traced in a narrow region on the pre-midnight near-Earth tail equatorial plane: X = −7.75 to −8.25 R_E and Y = 1.0 to 2.0 R_E. The scale length of each bead segment in the Y direction is 500–800 km, while the separation between the longitudinally arrayed beads is ∼1000 km. The scale of the beads and their separation are typically on the order of the gyroradius of 1–10 keV protons in the source magnetosphere. Thus, as suggested by *Liang et al.* [2008] and *Sakaguchi et al.* [2009], the plasma instability creating the beads in the primary stage of their development would not be a pure MHD scale process but include kinetic effect.

[12] During the current interval, the auroral beads showed a characteristic two-step evolution. In particular, the slowly moving beads in the first stage have never been reported in previous studies [*Donovan et al.*, 2006; *Sakaguchi et al.*, 2009]. Very recently, *Kataoka et al.* [2011], using an electron multiplier charge-coupled device (EMCCD) camera with a narrow FOV, demonstrated that smaller-scale auroral forms (on a scale of a few/several km) appear in a breakup arc in a few minutes before onset. They showed that the auroral forms undergo a two-step evolution: in the first few minutes the turbulent microstructures appear with a slow propagation speed (0.5–2.0 km s^{-1}), and subsequently they evolve into larger scale, brighter fold structures with a faster propagation speed (2.0–6.0 km s^{-1}). Such a two-step evolution from the slower-moving auroral structure to the faster-moving one resembles the event we observed, although their spatial scale and structure were quite different from the beads in the present study.

[13] We have presented a case in which auroral beads appeared with remarkable similarities in both northern and southern hemispheres. Such interhemispheric similarities provide strong evidence that the temporal evolution of the beads in the initial brightening arc is dominated by a driver in the magnetotail equatorial region, such as ballooning type instabilities. In other words, the auroral beads would remotely represent the evolution of the pre-onset magnetospheric process as a "screen projection" onto the conjugate ionospheres. In this paper, we focus only on the similarities between the auroral beads in both hemispheres. As shown in Figure 3, however, the characteristics of the beads in Iceland and Syowa were not always completely identical. This may imply that processes in the M-I coupling region can induce additional interhemispheric differences in the beads' behavior. We cannot discard such a possibility, because there are interhemispheric differences in the magnetic field intensity and ionospheric conductance between Iceland and Syowa. The magnitude of the magnetic field is 1.2 times larger in Iceland (|B| ∼52500 nT) than in Syowa (|B| ∼43000 nT). The ionospheric Pedersen conductance calculated from the IRI 2007 [*Bilitza and Reinisch*, 2008] and NRLMSISE-00 models [*Picone et al.*, 2002] was about 1.5 times larger in Syowa (0.112 S) than in Iceland (0.076 S) during the time interval studied in this paper. Such interhemispheric differences in the characteristic parameters in the M-I coupling processes probably prevented complete conjugacy in the behavior of the auroral beads, a hypothesis that will be studied in detail in our future research.

[14] **Acknowledgments.** This work was partially supported by a Grant-in-Aid for Scientific Research B (21403007) and the Inter-university Upper atmosphere Global Observation NETwork (IUGONET) project funded by the Ministry of Education, Culture, Sports, Science and Technology of Japan. The production of this paper was supported by an NIPR publication subsidy. Ground-based observations in Iceland were conducted by an international collaboration between the National Institute of Polar Research (NIPR), Japan, and the University of Iceland, Iceland. Special thanks are due to the 52nd Japanese Antarctic Research Expedition (JARE) members for carrying out the optical operation at Syowa Station. The THEMIS FGM data were obtained through the CDAWeb (http://cdaweb.gsfc.nasa.gov/). The provisional AU and AL indices were obtained from WDC for geomagnetism, Kyoto.

[15] The Editor thanks Petri Toivanen and an anonymous reviewer for assisting with the evaluation of this paper.

References

Akasofu, S.-I. (1964), The development of the auroral substorm, *Planet. Space Sci.*, *12*, 273–282, doi:10.1016/0032-0633(64)90151-5.

Auster, H. U., et al. (2008), The THEMIS fluxgate magnetometer, *Space Sci. Rev.*, *141*, 235–264, doi:10.1007/s11214-008-9365-9.

Bilitza, D., and B. W. Reinisch (2008), International Reference Ionosphere 2007: Improvements and new parameters, *Adv. Space Res.*, *42*, 599–609, doi:10.1016/j.asr.2007.07.048.

Chaston, C. C., and K. Seki (2010), Small-scale auroral current sheet structuring, *J. Geophys. Res.*, *115*, A11221, doi:10.1029/2010JA015536.

Cheng, C. Z. (2004), Physics of substorm growth phase, onset, and dipolarization, *Space Sci. Rev.*, *113*, 207–270, doi:10.1023/B:SPAC.0000042943.59976.0e.

Donovan, E. F., S. Mende, B. Jackel, M. Syrjäsuo, M. Meurant, I. Voronkov, H. U. Frey, V. Angelopoulos, and M. Connors (2006), The azimuthal evolution of the substorm expansive phase onset aurora, in *Proceedings of International Conference on Substorms-8*, edited by M. Syrjäsuo and E. Donovan, pp. 55–60, Univ. of Calgary, Calgary, Alberta, Canada.

Elphinstone, R. D., et al. (1995), Observations in the vicinity of substorm onset: Implications for the substorm process, *J. Geophys. Res.*, *100*, 7937–7969, doi:10.1029/94JA02938.

Henderson, M. G. (2009), Observational evidence for an inside-out substorm onset scenario, *Ann. Geophys.*, *27*, 2129–2140, doi:10.5194/angeo-27-2129-2009.

Kataoka, R., Y. Miyoshi, T. Sakanoi, K. Shiokawa, and Y. Ebihara (2011), Turbulent microstructures and formation of folds in auroral breakup arc, *J. Geophys. Res.*, *116*, A00K02, doi:10.1029/2010JA016334.

Liang, J., E. F. Donovan, W. W. Liu, B. Jackel, M. Syrjäsuo, S. B. Mende, H. U. Frey, V. Angelopoulos, and M. Connors (2008), Intensification of preexisting auroral arc at substorm expansion phase onset: Wave-like disruption during the first tens of seconds, *Geophys. Res. Lett.*, *35*, L17S19, doi:10.1029/2008GL033666.

Lysak, R. L., and Y. Song (2002), Energetics of the ionospheric feedback interaction, *J. Geophys. Res.*, *107*(A8), 1160, doi:10.1029/2001JA000308.

Motoba, T., K. Hosokawa, N. Sato, A. Kadokura, and G. Bjornsson (2010), Varying interplanetary magnetic field By effects on interhemispheric conjugate auroral features during a weak substorm, *J. Geophys. Res.*, *115*, A09210, doi:10.1029/2010JA015369.

Picone, J. M., A. E. Hedin, D. P. Drob, and A. C. Aikin (2002), NRLMSISE-00 empirical model of the atmosphere: Statistical comparisons and scientific issues, *J. Geophys. Res.*, *107*(A12), 1468, doi:10.1029/2002JA009430.

Sakaguchi, K., K. Shiokawa, A. Ieda, R. Nomura, A. Nakajima, M. Greffen, E. F. Donovan, I. R. Mann, H. Kim, and M. Lessard (2009), Fine structures and dynamics in auroral initial brightening at substorm onsets, *Ann. Geophys.*, *27*, 623–630, doi:10.5194/angeo-27-623-2009.

Tsyganenko, N., and D. Stern (1996), Modeling the global magnetic field of the large-scale Birkeland current systems, *J. Geophys. Res.*, *101*(A12), 27,187–27,198, doi:10.1029/96JA02735.